Closed-loop adaptive optics with a single element for wavefront sensing and correction

Raúl Martínez-Cuenca,[1,2] Vicente Durán,[1,2,*] Justo Arines,[3,4] Jorge Ares,[4] Zbigniew Jaroszewicz,[5] Salvador Bará,[3] Lluís Martínez-León,[1,2] and Jesús Lancis[1,2]

[1]*GROC·UJI, Departament de Física, Universitat Jaume I, 12080 Castelló, Spain*

[2]*Institut de Noves Tecnologies de la Imatge (INIT), Universitat Jaume I, 12080 Castelló, Spain*

[3]*Departamento de Física Aplicada, Universidade de Santiago de Compostela, 15782 Compostela, Galicia, Spain*

[4]*Departamento de Física Aplicada, Universidad de Zaragoza, Zaragoza, Spain*

[5]*Institute of Applied Optics, Kamionkowska 18, 03-805 Warsaw, Poland, and National Institute of Telecommunications, Szachowa 1, 04-894 Warsaw, Poland*

Corresponding author: vduran@sg.uji.es

We propose a closed-loop adaptive optical arrangement based on a single spatial light modulator that simultaneously works as a correction unit and as the key element of a wavefront sensor. This is possible by using a liquid crystal on silicon display whose active area is divided into two halves that are respectively programmed for sensing and correction. We analyze the performance of this architecture to implement an adaptive optical system. Results showing a closed-loop operation are reported, as well as a proof of concept for dealing with aberrations comparable to those typically found in human eyes.   © 2011 Optical Society of America

OCIS codes: 010.1080, 230.3720, 230.6120.

Commonly used systems for adaptive optics (AO) are composed of two separate and well defined units, each of which is purpose-built in order to comply with an assigned task [1,2]. One of these units is a wavefront sensing device, typically a Hartmann-Shack sensor (HSS), which performs real-time measurements of wavefront aberrations. The second unit is usually a computer-controlled reconfigurable element, like a deformable mirror (DM) or a spatial light modulator (SLM), which is fed with correcting phase patterns calculated on the basis of the measured aberrations.

Several types of liquid crystal (LC) SLMs have been assayed for AO systems [3–6]. These devices offer a promising alternative to widely used DMs, particularly in ophthalmic applications. The principal feature of LC-SLMs is their high spatial resolution, several orders of magnitude greater than in the case of DMs. In addition, the effective stroke of LC modulators can be increased by the use of 2π wrapped phase distributions, enabling generation of phase profiles with local discontinuities. The major disadvantages of LC-SLMs are their low response time (especially in common nematic LCs) and the diffraction artifacts due to their pixelated structure. Also, LC modulators require the use of light with a well defined state of polarization. Part of the above limitations has been overcome with the arrival of the so-called liquid crystal on silicon (LCoS) displays, which are SLMs that operate in reflective mode and provide pixel pitches of ~10 micrometers, fill factors exceeding 90%, and refreshing frequencies up to 60 Hz [7]. The ability of LCoS displays to generate wavefront aberrations (WAs) for ophthalmic purposes has been recently tested [8].

Concerning wavefront sensors, a HSS can be implemented by codifying a Fresnel microlens array (MLA) onto an LC SLM placed just before a CCD [9]. This LC HSS enables a tunable focal length, so the sensor performance can be optimized according to the changing features of the wavefront under test. The use of a liquid lens inserted in a proper telecentric relay system makes possible to reconfigure the LC HSS without moving parts, which improves its versatility and adaptability [10].

The described dual behavior of an LC SLM can be exploited to simplify the basic architecture of AO systems. The idea is to combine these two basic units into a single one but of double use. To this end, the measurement and compensation processes should be temporally or spatially multiplexed. In the temporal approach, compensation patterns and MLAs are alternately implemented onto the SLM, so in one step the device is used for wavefront sensing, whereas in the next step it is converted into the compensating unit [11]. This possibility enables it to make an optimum use of the light energy and the spatial resolution of the SLM. The sequential operation suffers from dead times and a correct operation requires the duty time of the device to be significantly shorter than the timescale for changes in the wavefront.

The second option is based on the spatial division of the tasks. The idea of exploiting the high spatial resolution of an LCoS display has been recently applied to implement a binocular AO visual simulator [12]. In our present proposal, the active area of the SLM is divided into two parts, one working as a correction unit (CU) and the other as a wavefront sampling element, respectively. In contrast to the temporal multiplexing approach, this operation mode allows us to implement a continuous closed-loop AO scheme. The goal of this Letter is to discuss this possibility and analyze the features and limitations of the setup.

The general scheme of the proposed device is as follows. A light beam from a laser is collimated with the aid of a spatial filter placed in the focal plane of a lens. The width of the beam is controlled by means of a variable aperture located after the collimating lens. Controlled aberrations are introduced at this point. Figure 1 shows a sketch of the double pass scheme. The incoming light beam (LB) impinges onto the right
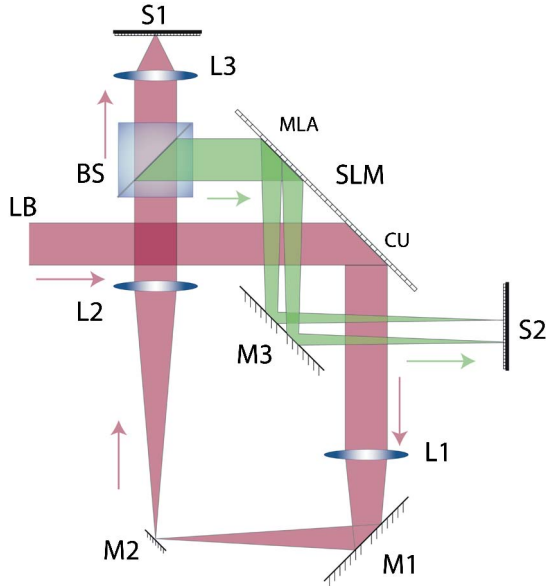
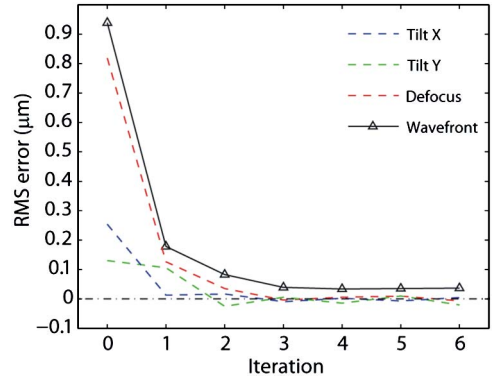Fig. 1. (Color online) Sketch of the double pass configuration.

Fig. 2. (Color online) Graph of the RMS wavefront error showing the convergence of the closed-loop operation. The RMS error curves for the Zernike terms corresponding to the tilt X, tilt Y and defocus are also included.

side of the modulator at an angle of 45°. Two lenses (not shown) form an image of the aberrated aperture onto this region of the LCoS display with a proper magnification. This is the half of the panel used as a CU. After reflection, the light passes through a set of two mirrors (M1, M2) and two lenses (L1, L2). A beam splitter divides the beam into two paths. The transmitted light is captured by the scientific camera composed of the CCD (S1) and the imaging lens (L3). The reflected beam impinges onto the MLA displayed at the left side of the modulator. If the two lenses L1 and L2 are identical and they are arranged in a $4f$ imaging system, an image of the wavefront on the CU is formed onto the MLA with unit magnification. A mirror M3 guides the light emerging from the MLA toward the CCD (S2). The ensemble MLA-S2 constitutes the HSS. Since the LCoS display works at non-normal incidence, the windows where the sensing and correction patterns are codified must be elliptical. In addition, the effect of the panel orientation over the codified phase functions must be taken into account [13].

The LC SLM used here is an LCoS display (Pluto model from HOLOEYE Photonics AG) with a panel size of 0.7 in., 1920×1080 pixels, a fill factor of 87%, and a pixel pitch of $8\,\mu m$. This display is specially designed for phase-only modulation, which is achieved when the input light is linearly polarized in a given direction. The modulator can be configured to achieve a phase depth of 2π radians at the laser wavelength (here, $\lambda = 543\,nm$). Pixels are individually addressed by sending gray-level images to the modulator. At normal incidence, the maximum diameter of the pupil that can be projected onto one half of the panel is $\sim 7.7\,mm$, which corresponds to a circular area containing ~ 0.72 megapixels.

The MLA codified on the left side of the panel was composed of 7×7 microlenses with a focal length of $36\,mm$, and a center-to-center spacing of $400\,\mu m$. Since the diameter of the system pupil was $\sim 3.5\,mm$, only 35 lenses were really employed for sampling. The focal spot patterns were recorded with the CCD S2. From the positions of the spot centroids, the aberrated wavefront was

estimated by fitting a Zernike expansion (up to and including the fifth radial order) to the sensor measurements [2]. The CU was initially switched off. In this way, the first HSS measurement provided not only the induced WAs but also the perturbations due to the own LC SLM, as well as to the other optical elements located along the light path. The point spread function (PSF) of the system was registered by the imaging CCD S1.

As a first evaluation of the proposed device, we studied the closed-loop operation by inserting a negative lens in the path of light to produce a certain amount of defocus. Figure 2 shows the value of the root-mean-square (RMS) error of the corrected wavefront after several iterations. The RMS of the incoming wavefront ($\sim 1.5\lambda$) corresponds to iteration 0, when the LCoS device simply acts as a mirror. The RMS error converges to a minimum value ($\sim\lambda/15$) after 3–4 corrections. This operation is comparable to that shown by reported LC-AO setups [2,5].

To illustrate the performance of our system to tackle higher order aberrations, we used an aberration plate besides the above lens. This plate was fabricated from a photoresist, which was deposited upon a glass substrate and exposed to UV radiation through a gray-level transmission mask [14]. To change the input aberration, the phase plate was rotated around its center. A set of measurements after inserting this element is presented in Fig. 3. Image I(a) shows the total PSF of the system, registered when the LCoS display was switched off. The WA measured in this case is shown in image I(b). The RMS error was 3.34λ. After that, the SLM was configured to display the corresponding correction pattern. The image at the CCD plane (PSF1) after one iteration is significantly improved, as can be observed in image I(c). Finally, image I(d) corresponds to the aberration that remained once the correction was done. The RMS error was reduced to $\lambda/2.4$. Next, we rotated the phase plate to get a new aberration while the SLM was displaying the previous correction. The new aberrated PSF is shown in image II(a). The system detected the residual aberration (RA1), which is the difference between the total aberration of the beam and the phase distribution WA previously codified on the SLM. The pattern corresponding to the phase WA plus the conjugate of RA1 is shown in image II(b). Its RMS error was 3.90λ. After displaying it onto the modulator, the registered intensity pattern
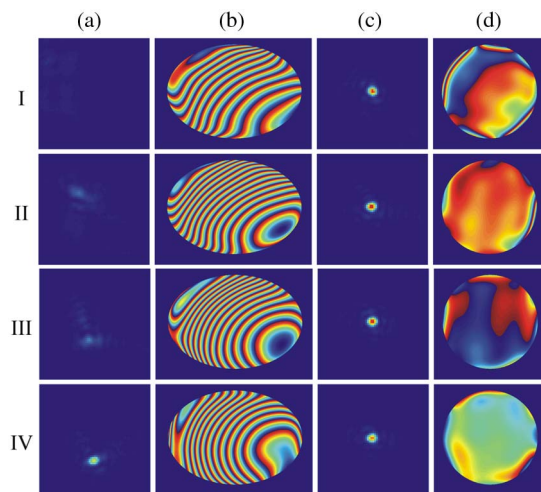
Fig. 3.   (Color online) Diagram to illustrate the performance of the proposed closed-loop AO system.

(PSF2) looked very similar to the previous one (PSF1), as can be observed in image II(c). The remaining aberration of the corrected PSF is shown in image II(d), with a RMS error of $\lambda/5.4$. Next, we rotated again the plate to get a new aberration and the whole process was repeated. Figure 3 shows in rows III and IV the corresponding images for other two positions of the aberration plate. The minimum RMS wavefront error ($\lambda/7.6$) was achieved for the image IV(d).

Now, let us describe the features and limitations of the proposed AO system and its potential applications. In any HSS there is a trade-off between the dynamic range and the measurement sensitivity. To deal with this trade-off, the MLA implemented on our display can easily adjust its geometry and focal length to optimize its performance. For example, with the lens size used here it is possible to codify lenslets with focal lengths from a minimum value of 6 mm. The range of focal lengths that can be employed in an adaptive LC-HSS is discussed in detail in [10]. By magnifying the system pupil, we could increase the number of lenses for wavefront sampling. This can be useful for ophthalmic applications, since the majority of high-order aberrations in a population of normal eyes is included in Zernike modes up to eighth order [15], and using an increased number of microlenses is advisable.

Concerning the CU, a frequent drawback of LC SLMs has been their limited phase modulation depth (see, for instance, [6]). In contrast, current LCoS displays can achieve a phase difference of 2π radians for any wavelength in the visible spectrum. Another aspect to consider is the upper limit of the phase slope that can be corrected by the display, which depends on the number of pixels N used to codify a complete phase period. Since an LC SLM acts as a diffractive element, a reduction of the number of phase levels per cycle (to increase the phase slope) leads to a drop in diffraction efficiency. For example, a four-level $[(0, \pi/2, \pi, 3\pi/2)\,\mathrm{rad}]$ encoding scheme ($N = 4$) enables the compensation of ~31 line pairs/mm in the aberration interferogram at 543 nm. Because of the fill factor, the light efficiency in this case

is 63%. If we extend the encoding scheme to eight levels, the maximum phase slope is reduced by one half but the light efficiency increases to 72%, and so on. In spite of this trade-off, the continuous improvement of the pixel pitch and fill factor of LCoS modulators (driven by the needs of the microdisplay industry) ensures results clearly superior to those presented in [6,11].

Finally, a key factor of a closed-loop AO system is its temporal bandwidth. The fundamental limitation for this parameter is the response time of the LC SLM. For current LCoS displays, the refreshing frequency reaches ~60 Hz. This value is usually reduced by other factors, like the rate of image acquisition or the computing time required by processing routines. However, with a suitable unit control it is possible to readily achieve frequencies of ~10 Hz, which are enough for addressing the main temporal dynamic characteristics of the human eye [2,5].

In conclusion, we have demonstrated an AO setup with a single LCoS display for wavefront sampling and correction operating in a closed-loop mode. In spite of the limitation of using narrow bandwidth light (with a well-defined polarization), our approach offers a compact and easily addressable AO setup when the required response time is relatively slow, like in visual optics.

References

1. R. K. Tyson, *Principles of Adaptive Optics* (Academic, 1998).
2. J. Porter, H. Queener, J. Lin, K. Thorn, and A. Awwal, *Adaptive Optics for Vision Science: Principles, Practices, Design and Applications* (John Wiley & Sons, 2006).
3. R. Dou and M. K. Giles, Opt. Lett. **20**, 1583 (1995).
4. G. D. Love, Appl. Opt. **36**, 1517 (1997).
5. P. M. Prieto, E. J. Fernández, S. Manzanera, and P. Artal, Opt. Express **12**, 4059 (2004).
6. V. Durán, V. Climent, E. Tajahuerce, Z. Jaroszewicz, J. Arines, and S. Bará, J. Biomed. Opt. **12**, 014037 (2007).
7. I. Moreno, A. Lizana, J. Campos, A. Márquez, C. Iemmi, and M. J. Yzuel, Opt. Lett. **33**, 627 (2008).
8. E. J. Fernández, P. M. Prieto, and P. Artal, Opt. Express **17**, 11013 (2009).
9. L. Seifert, J. Liesener, and H. J. Tiziani, Opt. Commun. **216**, 313 (2003).
10. R. Martínez-Cuenca, V. Durán, V. Climent, E. Tajahuerce, S. Bará, J. Ares, J. Arines, M. Martínez-Corral, and J. Lancis, Opt. Lett. **35**, 1338 (2010).
11. J. Arines, V. Durán, Z. Jaroszewicz, J. Ares, E. Tajahuerce, P. Prado, J. Lancis, S. Bará, and V. Climent, Opt. Express **15**, 15287 (2007).
12. E. J. Fernández, P. M. Prieto, and P. Artal, Opt. Lett. **34**, 2628 (2009).
13. E. Martín-Badosa, M. Montes-Usategui, A. Carnicer, J. Andilla, E. Pleguezuelos, and I. Juvells, J. Opt. A **9**, S267 (2007).
14. R. Navarro, E. Moreno-Barriuso, S. Bará, and T. Mancebo, Opt. Lett. **25**, 236 (2000).
15. J. Z. Liang, D. R. Williams, and D. T. Miller, J. Opt. Soc. Am. A **14**, 2873 (1997).